Distribution and trafficking of MPR300 is normal in cells with cholesterol accumulated in late endocytic compartments: evidence for early endosome-to-TGN trafficking of MPR300

Atsushi Umeda, Hideaki Fujita, Toshio Kuronita, Kaori Hirosako, Masaru Himeno, and Yoshitaka Tanaka[1]

Division of Pharmaceutical Cell Biology, Graduate School of Pharmaceutical Sciences, Kyushu University, 3-1-1 Maidashi, Fukuoka 812-8582, Japan

Abstract It has been reported that an accumulation of cholesterol within late endosomes/lysosomes in Niemann-Pick type C (NPC) fibroblasts and U18666A-treated cells causes impairment of retrograde trafficking of the cation-independent mannose 6-phosphate/IGF-II receptor (MPR300) from late endosomes to the *trans*-Golgi network (TGN). In apparent conflict with these results, here we show that as in normal fibroblasts, MPR300 localizes exclusively to the TGN in NPC fibroblasts as well as in normal fibroblasts treated with U18666A. This localization can explain why several lysosomal properties and functions, such as intracellular lysosomal enzyme activity and localization, the biosynthesis of cathepsin D, and protein degradation, are all normal in NPC fibroblasts. These results, therefore, suggest that the accumulation of cholesterol in late endosomes/lysosomes does not affect the retrieval of MPR300 from endosomes to the TGN. Furthermore, treatment of normal and NPC fibroblasts with chloroquine, which inhibits membrane traffic from early endosomes to the TGN, resulted in a redistribution of MPR300 to EEA1 and internalized transferrin-positive, but LAMP-2-negative, early-recycling endosomes.▪ We propose that in normal and NPC fibroblasts, MPR300 is exclusively targeted from the TGN to early endosomes, from where it rapidly recycles back to the TGN without being delivered to late endosomes. This notion provides important insights into the definition of late endosomes, as well as the biogenesis of lysosomes.—Umeda, A., H. Fujita, T. Kuronita, K. Hirosako, M. Himeno, and Y. Tanaka. **Distribution and trafficking of MPR300 is normal in cells with cholesterol accumulated in late endocytic compartments: evidence for early endosome-to-TGN trafficking of MPR300.** *J. Lipid Res.* **2003.** 44: 1821–1832.

Supplementary key words Niemann-Pick type C fibroblasts • endosomes • lysosomes • intracellular trafficking • *trans*-Golgi network • cation-independent mannose 6-phosphate/IGF-II receptor

Two distinct and related mannose 6-phosphate receptors (MPRs), the cation-dependent mannose 6-phosphate receptor (MPR46) and the cation-independent mannose 6-phosphate/IGF-II receptor (MPR300), are responsible for sorting soluble lysosomal enzymes from the secretory pathway. They have a largely overlapping but apparently distinct affinity for lysosomal enzymes (1, 2). Newly synthesized lysosomal enzymes acquire mannose 6-phosphate residues in the Golgi complex and are recognized in the *trans*-Golgi network (TGN) by MPRs [reviewed in refs. (3, 4)]. The ligand-receptor complex is subsequently packed into clathrin-coated vesicles and targeted to endosomal compartments. The acidic environment of endosomes causes the release of the enzymes from MRPs, after which the lysosomal enzymes are transferred to lysosomes while the MPRs are retrieved to the TGN for further rounds of sorting. Therefore, the MPRs play a key role in the biogenesis and function of lysosomes.

Intracellular trafficking of MPRs is mediated by signals present in their cytoplasmic tails, which contain two signals, tyrosine- and dileucine-based sorting signals, as well as by posttranslational modifications, such as the phosphorylation of serine residues and the palmitoylation of cysteine residues (3, 4). Notably, an acidic cluster-dileucine motif that consists of a cluster of acidic amino acid residues followed by dileucine residues is important to the sorting of MPRs from the TGN to endosomes. Recent progress in the study of MPR trafficking from the TGN to endosomes includes the finding of a novel family of sorting adaptors, Golgi-associated, γ-adaptin-homologous, ARF-interacting proteins (GGAs) [reviewed in refs. (5, 6)

and references therein]. The mammalian GGAs specifi-cally recognize the acidic cluster-dileucine motif of the MPRs and regulate the sorting and recruiting of MPRs into clathrin-coated transport vesicles from the TGN (7, 8).

Other MPR tail binding proteins, such as phosphofurin acidic cluster sorting protein 1 (PACS-1), AP-1, and TIP47, on the other hand, have been revealed to be in-volved in the retrieval of MPRs from endosomal compart-ments to the TGN [reviewed in ref. (5) and references therein]. It seems likely that PACS-1 and AP-1 cooperate in the retrieval, with PACS-1 functioning as a connector by linking the MPRs to AP-1 in the recycling of these recep-tors to the TGN (9). Indeed, the depletion of PACS-1 and AP-1 by an antisense oligonucleotide and gene disruption, respectively, causes a redistribution of MPR300 to endoso-mal compartments (10, 11). TIP47 also specifically inter-acts with the cytoplasmic tails of MPRs only on endosomal membranes (12), a process that is enhanced by Rab9 GTP-ase (13).

Several lines of evidence, further, have revealed the in-volvement of cholesterol in the transport of MPR300 from endosomes to the TGN (14–16). In a Chinese hamster ovary cell mutant, LEX2, that exhibits arrested endosomal carrier vesicle/multivesicular bodies (ECV/MVBs) (15), a reduction in the cellular free cholesterol level (about ~50% of control) causes the retention of MPR300 within ECV/MVBs (16). Restoration of the level allows the trans-port of the arrested MPR300 from the ECV/MVBs to the Golgi. These results suggest that cholesterol is required for the exit of MPR300 from ECV/MVBs. By contrast, in fibroblasts from patients with Niemann-Pick type C (NPC) disease, an autosomal recessive neurodegenerative lysoso-mal lipid storage disease characterized by a late endoso-mal/lysosomal accumulation of unesterified cholesterol derived from LDLs [reviewed in refs. (17, 18)], MPR300 is trapped in a compartment that has accumulated free cho-lesterol, a late endosomal marker lysobisphosphatidic acid (LBPA), and a late endosome/lysosome marker, LAMP-2 (14). Given the function of MPR300 as the receptor of ly-sosomal enzymes, such an alteration to its localization may result in the missorting of lysosomal enzymes. In fact, the redistribution of MPR300 from the TGN to endosomal compartments caused by a disruption of the gene for the μ1A subunit of AP-1 (11) or treatment with the phosphati-dylinositide 3-kinase inhibitor wortmannin (19–21) leads to an increase in secretion of a lysosomal enzyme, cathep-sin D.

Here we show that NPC fibroblasts have normal intra-cellular activity and lysosomal targeting of lysosomal en-zymes. Furthermore, evidence that MPR300 exhibits the same localization to the TGN in NPC fibroblasts as in nor-mal fibroblasts, but is not detected in cholesterol-loaded late endosomal/lysosomal compartments, indicates that the intracellular trafficking of MPR300 is not regulated by the accumulation of cholesterol within late endocytic compartments. Rather, this suggests that MPR300 is con-stitutively recycled between the TGN and early endosomes, bypassing a late endosomal compartment in both normal and NPC fibroblasts, which can explain why, in NPC fibro-blasts that exhibit impaired membrane trafficking from late endosomal/lysosomal compartments, MPR300 nor-mally localizes in the TGN.

EXPERIMENTAL PROCEDURES

Materials

Normal human skin fibroblasts (GM5565 and GM1652) and fibroblasts from patients with NPC disease (GM0110 and GM3123) were obtained from the Coriell Institute for Medical Research (Camden, NJ). Culture media and fetal calf serum were purchased from GIBCO BRL (Grand Island, NY). Filipin, 4-methylumbelliferyl-2-acetamido-2-deoxy-β-D-glucopyranoside, 4-methylumbelliferyl-α-D-mannopyranoside, 4-methylumbelliferyl-β-D-mannopyranoside, 4-methylumbelliferyl-β-D-glucuropyranoside, 4-methylumbelliferyl-β-D-galactopyranoside, and *p*-nitrocatechol sulfate were obtained from Sigma Chemical Co. (St. Louis, MO). Z-Phe-Arg-MCA was purchased from Peptide Institute Inc. (Osaka, Japan). Cy3-conju-gated human transferrin (Tfn), epidermal growth factor (EGF), and Alexa488- and Alexa594-labeled secondary antibodies were purchased from Molecular Probes (Eugene, OR). EXPRESS™ Protein Labeling Mix, [^{35}S]Easy Tag™, was obtained from New En-gland Nuclear (Boston, MA). Human recombinant EGF was pur-chased from Calbiochem (San Diego, CA). U18666A was ob-tained from Biomol (Plymouth Meeting, PA).

Cell culture

Normal and NPC fibroblasts were cultured in DMEM supple-mented with 20% FBS, 2 mM glutamine, and 1% penicillin-strep-tomycin in humidified 95% air and 5% CO_2 at 37°C. The cells were plated onto 13 mm coverslides the day before transfection. After 36 h, the cells were used for immunocytochemical experi-ments.

Antibodies

Mouse monoclonal antibodies to human LAMP-1 were ob-tained from the Developmental Studies Hybridoma Bank main-tained by the University of Iowa (Iowa City, IA). Mouse monoclo-nal antibodies to AP-1, EEA1, GM130, syntaxin 6, and the EGF receptor (EGFR) were purchased from Transduction Laborato-ries (Lexington, KY). Rabbit polyclonal antibodies to rat MPR300 were raised against either a fusion protein encoding glutathion *S*-transferase coupled to a portion of the cytoplasmic tail (amino acids 2,313 to 2,409) of rat MPR300 (22) or purified receptor from bovine liver by penta phosphomannan affinity chromatography as described previously (23). Mouse monoclonal antibody to the bovine MPR300 (MA1-066) was obtained from Affinity BioReagents (Golden, CO). Rabbit polyclonal antibodies to MPR46 were kindly provided by S. Höning and K. von Figura (Göttingen, Germany). Rabbit polyclonal antibodies to human cathepsin D were purchased from DAKO Co. (Carpinteria, CA).

Lysosomal enzyme assays

Normal and NPC fibroblasts cultured on 35 mm dishes were washed with PBS, scraped, and homogenized in PBS/0.1% Triton X-100. Lysosomal enzymes were detected using fluorometric as-says as described by Köster, von Figura, and Pohlmann (24). Aryl-sulfatase A was measured using *p*-nitrocatechol sulfate as substrate (25). Cathepsins B and L activities were assayed as described by Barret and Kirshke (26), using Z-Phe-Arg-MCA as the substrate.

Metabolic labeling and immunoprecipitation

For labeling with [^{35}S]methionine/cysteine, cells were first in-cubated in methionine/cysteine-free DMEM supplemented with

10% dialyzed fetal bovine serum for 30 min and then labeled in the same medium containing 100 μCi/ml EXPRE^{35}S^{35}S protein labeling mixture. The labeled cells were homogenized in 10 mM Tris-HCl (pH 7.4), containing 150 mM NaCl, 1% Triton X-100, 0.5% sodium deoxycholate, 1% BSA, 2 mM EDTA, and a protease inhibitor mixture, and centrifuged in a microfuge for 10 min to remove insoluble compounds. Cell extracts were immunoprecipitated with anti-human cathepsin D antibody and protein A-Sepharose as described previously (27, 28). The immunoprecipitates were analyzed by SDS-PAGE according to Laemmli (29) using 10% acrylamide under reducing conditions and were quantitated with a Fuji BAS 1000 Imaging Analyzer.

Immunofluorescence microscopy

Cells cultured on coverslips were rinsed with PBS, fixed immediately in 3% paraformaldehyde (PFA) in PBS (pH 7.4), for 30 min at room temperature, and permeabilized with 0.05% saponin in PBS for 15 min. Cells were quenched with 50 mM NH$_4$Cl in PBS for 15 min and blocked with 1% BSA in PBS for 30 min. They were then incubated for 1 h in blocking solution using the following dilutions of primary antibodies: anti-LAMP-2 antibody (1:100), anti-EEA1 antibody (1:100), anti-MPR300 antibody (1:100), anti-AP-1 antibody (1:100), anti-syntaxin 6 antibody (1:100), and anti-GM130 antibody (1:100). The cells were washed with blocking solution and incubated for 30 min with the secondary antibodies diluted in blocking solution. Coverslips were then washed five times with blocking solution, rinsed with water, and mounted onto glass slides. Fluorescence was viewed using a fluorescence light microscope (Leica DMRB; Wetzlar, Germany) and a 63× oil immersion lens. Photographic images were acquired using a cooled CCD camera (MicroMAX; Princeton Instruments, Trenton, NJ), processed using IPlab software (Scanalytics, Fairfax, VA), and merged using Adobe Photoshop software (Adobe Systems, Mountain View, CA). For some experiments, the cells were analyzed by confocal laser scanning microscopy using a Radiance 2100 MP confocal microscope (Bio-Rad Laboratories, Richmond, CA) with an argon/krypton laser, the Red Diode laser, and the Blue Diode laser.

Tfn internalization

For Tfn internalization, cells cultured on coverslips were incubated in serum-free DMEM with BSA (1 mg/ml) for 30 min and then with Cy3-labeled Tfn (25 μg/ml) for 1 h at 37°C. After internalization, cells were washed with PBS, fixed in 3% PFA in PBS, and permeabilized with saponin in PBS before being immunostained for MPR300.

Filipin staining

Cells cultured on coverslips were rinsed with PBS and fixed in 3% PFA in PBS (pH 7.4), for 30 min at room temperature. They were stained (and permeabilized) with 0.05% filipin in PBS for 1 h, then immunostained for several organelle markers.

Western blotting

Normal and NPC fibroblasts cultured on 35 mm dishes were washed with PBS, scraped, and homogenized in PBS-0.1% Triton X-100. Next, 100 μg of protein was subjected to SDS-PAGE (5% polyacrylamide in the case of MPR300; 10% in the case of MPR46 and cathepsin D) under reducing conditions. Proteins were transferred to a polyvinylidene difluoride membrane (Schleicher and Schüll, Dassel, Germany), which was subsequently blocked with 10 mM PBS (pH 7.4), 0.05% Triton X-100, and 5% milk-powder (blocking buffer) for 1 h at room temperature. The blot was incubated overnight at 4°C with rabbit anti-human cathepsin D, anti-MPR46, or anti-MPR300 antibody, then washed with 10 mM PBS-0.1% Triton X-100. Subsequently, incu-

bation with horseradish peroxidase-coupled goat anti-rabbit antibody was performed for 1 h at room temperature followed by washing with 10 mM PBS-0.1% Triton X-100. Blots were finally analyzed using the ECL Detection System (Amersham Pharmacia Biotech).

EGF-induced EGFR degradation

Both normal and NPC fibroblasts were incubated for 16 h with DMEM containing 1% BSA, after which they were incubated with 500 ng/ml of hEGF for a given period. Cells were harvested with 10 mM Tris-HCl (pH 7.4), 0.15M NaCl, and 0.1% Triton X-100 and 100 μg of each sample was subjected to SDS-PAGE using 7.5% acrylamide under reducing conditions. Proteins were transferred to a polyvinylidene difluoride membrane, and EGFR was detected with anti-hEGFR antibody followed by the ECL Detection System. The bands were quantitated using NIH-image.

RESULTS

NPC fibroblasts have normal levels of intracellular lysosomal enzyme activities, except for β-mannosidase

The previous finding that MPR300, which is normally distributed in the TGN, was largely redistributed from the TGN to CD63-positive late endosomes in NPC fibroblasts (14) led us to speculate that the loss of MPR300 from the TGN would cause the missorting of many lysosomal enzymes to the culture medium, leading to a reduction in intracellular enzyme activities. To examine this possibility, we measured several lysosomal enzyme activities in NPC fibroblasts and compared them with those in normal fibroblasts. We found that in NPC fibroblasts, most of the lysosomal enzyme activities tested here were indistinguishable from those in normal fibroblasts (**Fig. 1**). Although in this study, we used two different cell lines, normal and NPC fibroblasts, all lysosomal enzymes measured had almost the same levels of activity in each cell line. Moreover, there was no difference in amounts of lysosomal enzymes secreted between normal and NPC fibroblasts (**Fig. 2**), suggesting that in NPC fibroblasts, these lysosomal enzymes were effectively targeted to lysosomes.

It has been reported that in NPC fibroblasts, sphingomyelinase, glucocerebrosidase, and β-glucosidase activities are reduced by around 40% to 50% (30, 31). We also observed about a 50% reduction of β-glucosidase activity in NPC fibroblasts compared with normal fibroblasts (data not shown). It should be noted that in NPC fibroblasts, β-mannosidase activity was reduced to ~40% compared with normal fibroblasts (Fig. 1). This reduction was not due to an enhanced secretion (Fig. 2). Furthermore, elevated cholesterol levels in late endosomes/lysosomes on treatment of normal fibroblasts with U18666A did not influence β-mannosidase activity (data not shown). Therefore, β-mannosidase may be one of the enzymes affected by a mutation of NPC1. It will be further necessary to determine whether the transfection of NPC1 or β-mannosidase back into NPC fibroblasts can elevate β-mannosidase activity or rescue the phenotypes affected by a mutation of NPC1.

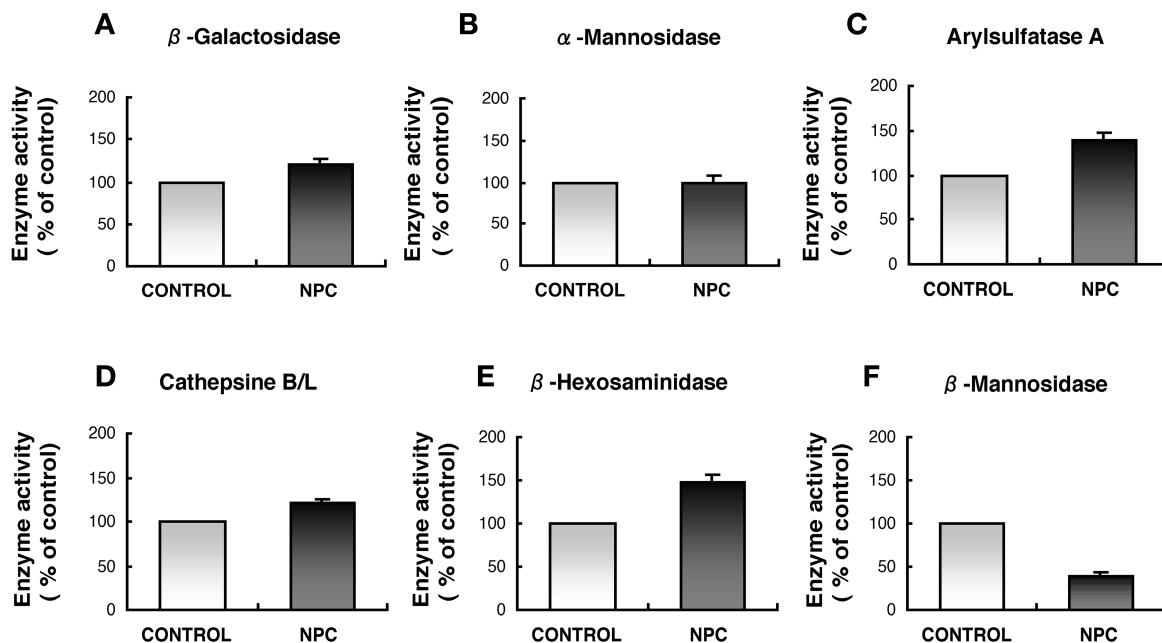In contrast to MPR46, MPR300 can recapture lysosomal enzymes missorted extracellularly at the cell surface and

Fig. 1. Lysosomal enzyme activities in normal and Niemann-Pick type C (NPC) fibroblasts. The activity of β-galactosidase (A), α-mannosidase (B), arylsulfatase A (C), cathepsin B/L (D), β-hexosaminidase (E), and β-mannosidase (F) was determined in normal and NPC fibroblasts. Error bars represent means ± SE (n = 5).

deliver them to endosomal compartments (4). An alternative explanation is, therefore, that the normal lysosomal enzyme activities in NPC fibroblasts might come from an enhanced recapture of the secreted enzymes by MPR300 expressed on the cell surface. To examine this possibility, 5 mM mannose 6-phosphate was added to the cultured medium to prevent further internalization of the secreted lysosomal enzymes via MPR300. The result was that there was no effect on the distribution of enzyme activities between cell lysate and medium in either normal or NPC fi-
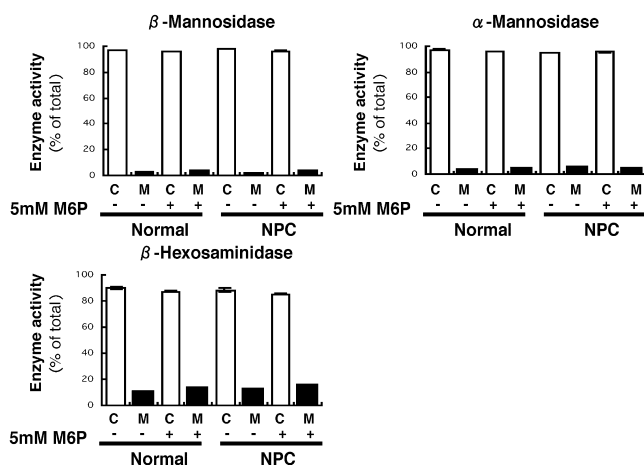

Fig. 2. Effect of mannose 6-phosphate on the secretion of lysosomal enzymes. Normal and NPC fibroblasts were incubated for 24 h in the absence or presence of 5 mM mannose 6-phosphate. Activities of three lysosomal enzymes, β-mannosidase, β-hexosaminidase, and α-mannosidase, were determined in cells and media. The activity in the secretion as a percentage of total activity is given, as well as the range of values in two culture dishes processed in parallel.

broblasts (Fig. 2). Thus, MPR300-dependent lysosomal enzyme targeting appears to be normal in NPC fibroblasts. In addition, immunoblot analysis and pulse-chase experiments using [^{35}S]methionine/cysteine showed that there is no difference in the amounts and processing of cathepsin D between normal and NPC fibroblasts (**Fig. 3A**, **B**). Furthermore, there was no increase in the secretion of procathepsin D in NPC fibroblasts, indicating that the newly synthesized cathepsin D was effectively targeted to lysosomes. Immunocytochemical data from triple labeling using antibodies for cathepsin D and LAMP-1 and filipin for cholesterol revealed that in NPC fibroblasts, cathepsin D extensively colocalizes with LAMP-1 and cholesterol in late endosomal/lysosomal compartments (Fig. 3C) confirming the normal targeting and localization of lysosomal enzymes to late endosomes/lysosomes in NPC fibroblasts.

MPR300 localizes primarily in the TGN in both normal and NPC fibroblasts

The normal targeting of lysosomal enzymes in NPC fibroblasts led us to consider the possibility that MPR300 may be localized in the TGN, a site that functions as a receptor for lysosomal enzymes. We then examined the intracellular distribution of MPR300 in both normal and NPC fibroblasts by triple labeling with several well-known organelle markers, GM130 for a *cis*-Golgi marker, AP-1 and syntaxin 6 for a TGN marker, EEA1 for an early endosome marker, LAMP-1 or LAMP-2 for a late endosome/lysosome marker, and filipin for free cholesterol. We used in this experiment antibodies against the cytoplasmic tail of MPR300. This antibody was found to react with many cell lines, such as COS (22), HeLa, U251, MDCK, and NRK cells (data not shown) and displayed TGN-like staining in all cell lines tested. As shown in **Fig. 4A–E**, in nor-
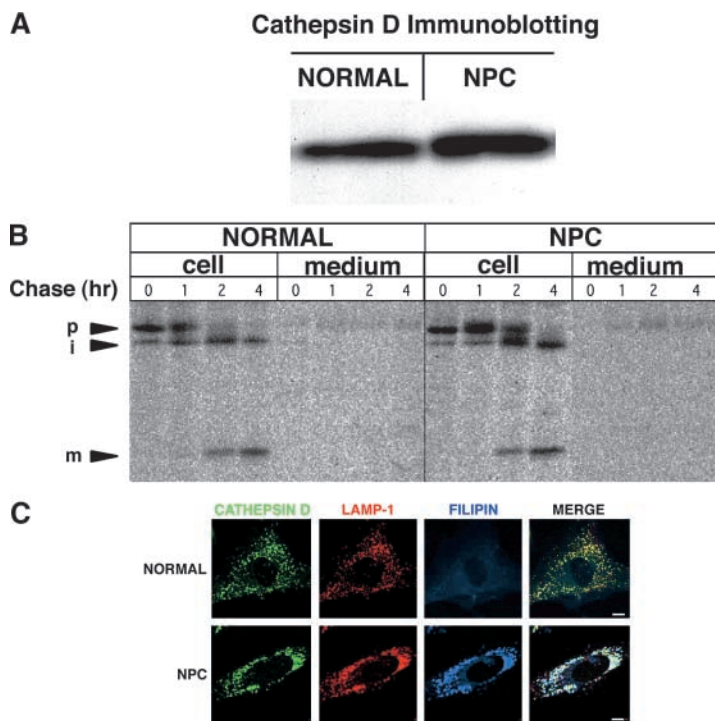
Fig. 3. Biosynthesis and localization of cathepsin D in normal and NPC fibroblasts. A: Western blotting of cathepsin D from normal and NPC fibroblasts. Each 100 μg of cell lysate from normal and NPC fibroblasts was subjected to SDS-PAGE, followed by Western blot analysis for cathepsin D. The mature form of 33 kDa was detected in both fibroblasts. B: Immunoprecipitation of cathepsin D. Normal and NPC fibroblasts were labeled with [^{35}S]methionine/cysteine for 30 min and then chased as indicated. Cathepsin D was immunoprecipitated from the cells and medium. In normal and NPC fibroblasts, cathepsin D was synthesized as a precursor form having a molecular weight of 53 kDa (p), and subsequently processed to a 33 kDa mature form (m) via a transient intermediate form of 44 kDa (i). A small amount of precursor form was secreted into the medium in both normal and NPC fibroblasts. C: Intracellular localization of cathepsin D. Normal and NPC fibroblasts were fixed, permeabilized, and stained with anti-cathepsin D (green), anti-LAMP-2 (red), and filipin for cholesterol (cyan). Cells were visualized by confocal microscopy. The right columns show the merged image for cathepsin D, LAMP-2, and cholesterol. Bars = 10 μm.

mal fibroblasts, MPR300 staining was seen as reticular, and small punctate structures around the perinuclear region and never colocalized with LAMP-1 (Fig. 4A). Although the perinuclear localization of MPR300 well resembled that of GM130, the two did not completely overlap. A significant overlapping was observed on double labeling with two TGN markers, AP-1 and syntaxin 6 (Fig. 4D, E), thereby indicating that the primary localization of MPR300 is in the TGN. Also, only a small fraction of MPR300-positive vesicle-like structures occasionally colocalized with EEA1 (Fig. 4B). As expected, the distribution of MPR300 in NPC fibroblasts was undistinguishable from that in normal fibroblasts. Consistent with the staining pattern in normal fibroblasts, MPR300 colocalized extensively with AP-1 and syntaxin 6 and partially with EEA1 in NPC fibroblasts (Fig. 4B, D, E). In contrast to the previous result (14), even in NPC fibroblasts, MPR300 was not localized to large LAMP-1-positive vacuolar compartments where free cholesterol is accumulated, as evidenced by the filipin staining (Fig. 4A). Taken together, these results clearly indicate that as in normal fibroblasts in NPC fibroblasts, MPR300 is primarily distributed in the TGN, not in the cholesterol-laden late endosomes/lysosomes.

We cannot rule out the possibility, however, that the difference in the distribution of MPR300 observed between this and other studies (14) may be due to a difference in cell lines or antibodies used. However, we observed the localization of MPR300 to the TGN in normal and NPC fibroblasts using two different cell lines of each (data not shown) and three different antibodies for MPR300 (**Fig. 5**): a polyclonal antibody raised against the cytoplasmic tail of MPR300 (as shown in Fig. 4); a polyclonal antibody raised against purified bovine MPR300; and a mouse monoclonal antibody for the bovine MPR300, which rec-

ognizes an epitope in the extracellular domain of MPR300. Indeed, double staining used the polyclonal antibody against the cytoplasmic tail or purified receptor and the monoclonal antibody showed almost overlapping staining (Fig. 5). Moreover, like MPR300, MPR46 displayed colocalization with AP-1, but not with LAMP-1, in both normal and NPC fibroblasts (**Fig. 6**), indicating that MPR46 also distributes to the TGN independently of the accumulation of cholesterol within late endosomes/lysosomes.

Cholesterol-laden late endosomes/lysosomes in NPC fibroblasts are degradative compartments

It has been demonstrated that the cytoplasmic tails of MPR46 and MPR300 contain a signal that is required to prevent transport of the receptors to lysosomes and subsequent lysosomal degradation (12, 32). The redistribution of MPR300 to late endocytic compartments in NPC fibroblasts reported previously by Kobayashi et al. (14) may imply that these compartments have less proteolytic activity in NPC fibroblasts than in normal fibroblasts, thereby leading to accumulation of MPR300. Immunoblot analysis, however, showed that the steady-state level of both MPR46 and MPR300 in NPC fibroblasts was the same as that in normal fibroblasts (**Fig. 7**). Furthermore, we found that lysosomal protein degradation in NPC fibroblasts is normal, based on EGF-induced EGFR degradation. As shown in **Fig. 8**, in normal fibroblasts, more than 80% of EGFR was degraded following stimulation with EGF for 4 h. Similarly, the same amount of EGFR was degraded in NPC fibroblasts. Furthermore, starvation-induced autophagic degradation of long-lived proteins was also normal in NPC fibroblasts (data not shown). Altogether, the normal degradative functions of late endosomal/lysosomal com-
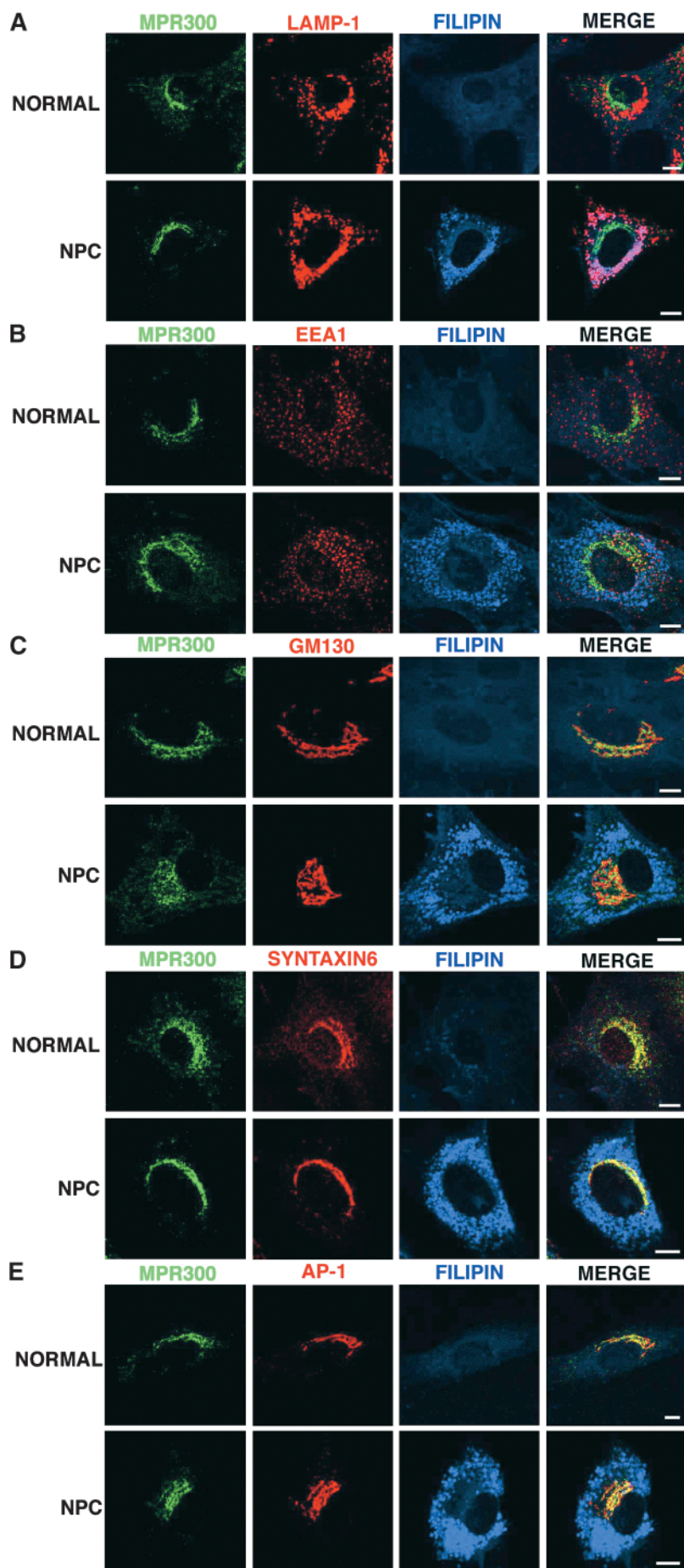
Fig. 4. Localization of the cation-independent mannose 6-phosphate/IGF-II receptor (MPR300) in normal and NPC fibroblasts. Normal and NPC fibroblasts were fixed, permeabilized, and incubated with primary antibodies to MPR300 (A–E, green) and LAMP-2 (A, red), EEA1 (B, red), GM130 (C, red), syntaxin 6 (D, red), or AP-1 (E, red) together with filipin for staining free cholesterol (A–E, cyan). The primary antibodies were revealed by incubation with either Alexa488-conjugated anti-rabbit immunoglobulin or Cy3-conjugated anti-mouse immunoglobulin secondary antibodies. Cells were visualized by confocal microscopy. The right columns show the merged images of triple staining of MPR300, each organelle marker, and cholesterol. Bars = 10 μm.
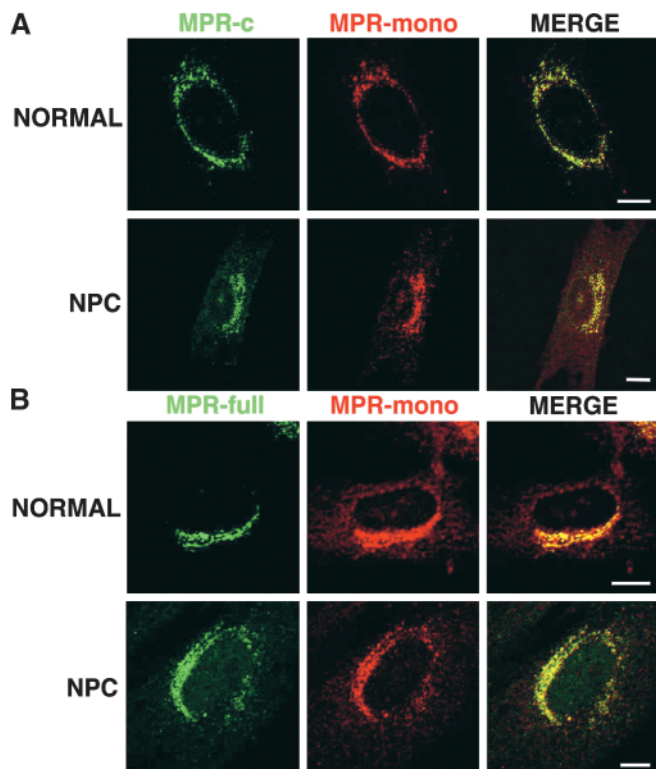
Fig. 5. The *trans*-Golgi network (TGN) localization of MPR300 in normal and NPC fibroblasts does not depend on antibodies. Normal and NPC fibroblasts were fixed, permeabilized, and immunostained with monoclonal antibodies against MPR300 and polyclonal antibodies against the cytoplasmic tail (A) or purified MPR300 (B). Cells were visualized by confocal microscopy. The right columns show the merged images of monoclonal antibodies (red) and each polyclonal antibody (green). Bars = 10 μm.

partments in NPC fibroblasts cannot explain the accumulation of MPR300 in these compartments.

Treatment with U18666A does not alter the TGN localization of MPR300

U18666A prevents cholesterol efflux out of late endosomes/lysosomes and thereby mimics the NPC cellular lesion (33). Previous study has further shown that U18666A treatment causes the redistribution of MPR300 from the TGN to LAMP-1-positive compartments (14). In contrast, our immunofluorescence data presented above apparently indicated that MPR300 localizes predominantly in the TGN, not only in normal fibroblasts but also in NPC fibroblasts despite the abundance of cholesterol in LAMP-1-positive late endosomes/lysosomes. Therefore, we further examined in normal fibroblasts treated with U18666A whether the cholesterol accumulated into late endosomes/lysosomes affects the intracellular distribution of MPR300. When normal fibroblasts were treated with 7 μM U18666A for 48 h and stained for unesterified cholesterol with filipin, a marked intracellular accumulation of cholesterol reminiscent of that in NPC fibroblasts was seen (**Fig. 9**), consistent with the effect of U18666A reported so far (33). Indeed, most of the cholesterol-loaded vacuoles were well colocalized with the late endosome/

lysosome marker LAMP-1 (Fig. 9), thereby indicating the accumulation of free cholesterol in late endosomes/lysosomes. Nevertheless, the distribution of MPR300 in fibroblasts treated with U18666A was significantly undistinguishable from that in untreated fibroblasts (Fig. 4). Moreover, MPR300 exclusively colocalized with syntaxin 6 even in U18666A-treated fibroblasts (Fig. 9) as in untreated fibroblasts. Taken together, these findings clearly indicate that the accumulation of free cholesterol in late endosomes/lysosomes does not affect the distribution of MPR300. This was also supported by the finding that most of the lysosomal enzyme activity in fibroblasts treated with U18666A was comparable to that in normal fibroblasts (data not shown). The same result was obtained with U18666A-treated normal rat kidney cells (data not shown). These results, therefore, demonstrate that cholesterol accumulation within late endosomal/lysosomal compartments does not affect the localization of MPR300 to the TGN.

Chloroquine treatment of normal and NPC cells causes the redistribution of MPR300 to early endosomes

It should be noted that in NPC fibroblasts, there was no significant accumulation of free cholesterol in early endosomes, thereby suggesting that the membrane traffic through early endosomes is not significantly affected in NPC fibroblasts. This is also supported by the normal morphology of early endosomes in NPC fibroblasts (Fig. 4B). Indeed, it has been considered that perturbation of the membrane traffic in NPC fibroblasts occurs primarily in the late endocytic pathway (34–36), as evidenced by the abnormal late endosomal/lysosomal accumulation of cholesterol, which is normally targeted to the cell surface and the endoplasmic reticulum. These lines of evidence, together with the TGN localization of MPR300 in NPC fibroblasts, led us to speculate, therefore, that MPR300 recycles between the TGN and early endosomes without traversing late endocytic compartments where free cholesterol is accumulated, due to mutation in the NPC1 gene or treatment with U18666A. To demonstrate this possibility, we examined the effect of chloroquine on the distribution of MPR300. Chloroquine treatment of cells has been known to impair the membrane traffic from early endosomes and to cause swelling of the endocytic compartments, including late endosomes and lysosomes (37, 38). In this case, TGN38, which recycles between the TGN and the cell surface via early endosomes, is accumulated in early endosomes in the chloroquine-treated cells. Therefore, if MPR300 follows the same route as TGN38, chloroquine treatment would cause MPR300 to become trapped in early endosomes. Chloroquine treatment resulted in an alteration of the subcellular distribution of MPR300 from the TGN to small vesicular structures scattered around the perinuclear region in both normal and NPC fibroblasts (**Fig. 10**). Although chloroquine treatment of both fibroblasts also resulted in swelling of LAMP-1-positive late endosomes/lysosomes, MPR300 was never detected in these compartments (Fig. 10A). As expected, in normal and NPC fibroblasts, MPR300-positive vesicular structures induced by
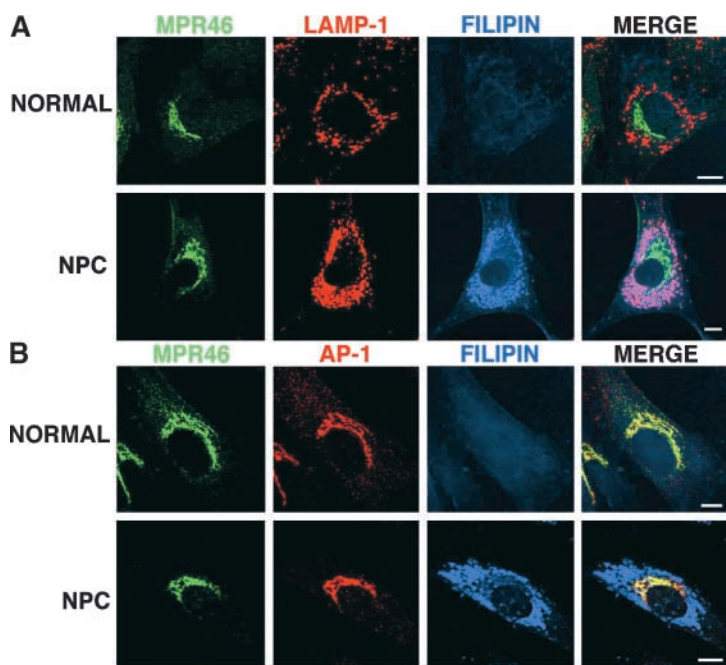
Fig. 6. Cation-dependent mannose 6-phosphate receptor (MPR46) also localizes in the TGN. Normal and NPC fibroblasts were fixed, permeabilized, and incubated with primary antibodies to MPR46 (A and B, green) and LAMP-1 (A, red) or AP-1 (B, red), together with filipin for staining free cholesterol (A and B, cyan). The primary antibodies were revealed by incubation with either Alexa488-conjugated anti-rabbit immunoglobulin or Cy3-conjugated anti-mouse immunoglobulin secondary antibodies. Cells were visualized by confocal microscopy. The right columns show the merged images for triple staining of MPR46, each organelle marker, and cholesterol. Bars = 10 μm.

chloroquine treatment were found to have characteristics of early endosomes, because both EEA1 and internalized Cy3-labeled Tfn, which recycles back to the cell surface via early endosomes after endocytosis, colocalized with MPR300 in these vesicular structures (Fig. 10C, D). Thus, the retention of MPR300 in early endosomes after chloroquine treatment could be attributed to impairment of the membrane traffic from early endosomes to the TGN, as demonstrated previously (37, 38). The same results were obtained in other cell lines, such as NRK and rat 3Y-1B cells (data not shown). These results, therefore, suggest that MPR300 continuously travels between the TGN and early endosomes, which can explain why in NPC fibroblasts that exhibit a defect in membrane traffic from late endosomal/lysosomal compartments, MPR300 localizes to the TGN.

in NPC fibroblasts. We also provide evidence that the accumulation of cholesterol within late endosomes/lysosomes triggered by the mutation of NPC1 or U18666A treatment does not cause a redistribution of MPR300 from the TGN to these compartments, in apparent conflict with previous results reported by Kobayashi et al. (14). Thus, the late endosomal/lysosomal cholesterol accumulation-independent localization of MPR300 appears to reflect normal endosome-to-TGN trafficking of MPR300 in cells loaded with cholesterol in late endocytic compartments such as NPC fibroblasts.

This notion is further supported by our recent findings. We found that overexpression of the lysosomal membrane protein, LGP85, in COS cells causes the enlargement of

DISCUSSION

We show here that the lysosomal functions tested, such as intracellular activity, localization, and biosynthesis of lysosomal enzymes and protein degradation were normal
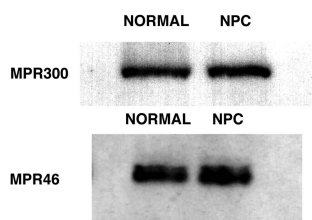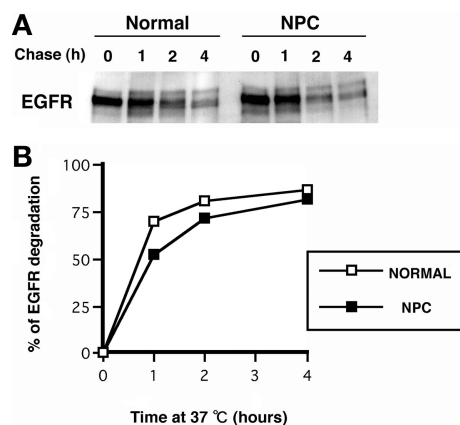

Fig. 7. Immunoblot analysis of MPR300 in normal and NPC fibroblasts. Western blotting of MPR300 and MPR46 from normal and NPC fibroblasts. Each 100 μg of cell lysate from normal and NPC fibroblasts was subjected to SDS-PAGE, followed by Western blot analysis for MPR300 and MPR46.

Fig. 8. Epidermal growth factor (EGF)-induced EGF receptor (EGFR) degradation in normal and NPC fibroblasts. Normal and NPC fibroblasts were serum starved, then incubated for 1 h with EGF (100 ng/ml) at 4°C, and warmed to 37°C for up to 4 h. After the indicated period, each cell was subjected to SDS-PAGE, followed by Western blot analysis for EGFR (A). Equal amounts of protein were loaded in each lane. The bands were quantitated by densitometry (B).
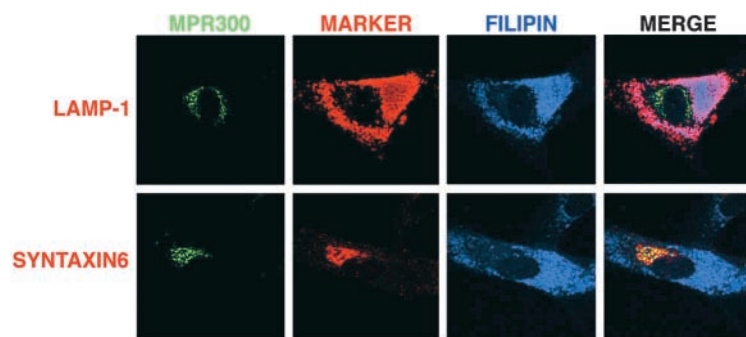
Fig. 9. Treatment of normal fibroblasts with U18666A causes accumulation of cholesterol in late endosomes/lysosomes, but does not affect the TGN localization of MPR300. Normal and NPC fibroblasts were incubated for 24 h in the absence or presence of 7 μM U18666A. Cells were then fixed, permeabilized, and incubated with anti-MPR300 (green) and anti-LAMP-1 (red) or anti-syntaxin 6 (red) together with filipin (cyan). Cells were visualized by confocal microscopy. The right columns show the merged images for triple staining of MPR300, each organelle marker, and cholesterol.

early endosomes and late endosomes/lysosomes (22). These enlarged compartments have free cholesterol, and the membrane traffic out of these was severely impaired, reminiscent of the phenotypes observed in NPC fibroblasts. Nevertheless, the steady-state distribution of MPR300 was exclusively restricted to the TGN. In addition, Frolov et al. (39) have recently created a novel mutant cell harboring NPC-like phenotypes (accumulation of unesterified cholesterol in late endosomes/lysosomes), but with a mutation in a gene distinct from *NPC1* and *NPC2*, and have shown that MPR300 does not localize to a compartment that is enriched in cholesterol and LAMP-2. Together with the data presented here, these results therefore lead to the conclusion that the accumulation of cholesterol within endosomal/lysosomal compartments does not affect the steady-state distribution of MPR300.

The results presented here do not necessarily imply that cholesterol itself is not implicated in the regulation of transport of MPR300. It has been reported that 50–100% of normal cellular free cholesterol is needed for the retrograde transport of MPR300 from endosomal compartments to the TGN (16). It still remains to be elucidated, however, how the retrieval of MPR300 from endosomal compartments to the TGN is regulated by cellular cholesterol levels. The previous result on the redistribution of MPR300 to late endosomal compartments upon the treatment of cells with U18666A also suggests that the late endosomal accumulation of MPR300 is a consequence, rather than a cause, of elevated levels of cholesterol, as the redistribution of MPR300 occurred more slowly than the accumulation of cholesterol in late endosomes (14). The authors have further revealed that the antibody-mediated disruption of negatively charged lipid LBPA function causes the accumulation of MPR300 and cholesterol in internal membranes within late endosomal compartments, resembling the phenotypes of NPC fibroblasts (40). Indeed, treatment of cells with U18666A can also induce accumulation of cholesterol and LBPA in the late endocytic compartments (14). Consistent with these results, we observed the accumulation of LBPA within cholesterol-laden late endosomal compartments in both NPC fibroblasts and cells treated with U18666A, whereas this treatment did not lead to the redistribution of MPR300 to LBPA-positive compartments (data not shown). It has been suggested that NPC1 may be the target of U18666A, because overexpression of NPC1 suppressed the effects of the

drug (41). Recent evidence has shown that NPC1 localizes in a subset of late endosomal compartments positive for LAMP-2 and Rab7 but negative for MPR300 (34, 42), and moves from this compartment by a dynamic process involving tubulation and fission, which is modulated by cholesterol content, thereby reflecting the possible function of NPC1 in cholesterol clearance from endosomal membranes (43, 44). Interestingly, recent studies have demonstrated that overexpression of wild-type Rab9 or Rab7 in NPC fibroblasts restores Golgi targeting of glycosphingolipid and dramatically reduces the accumulation of intracellular cholesterol (45), though such an effect of Rab7 is still controversial (46).

Our interpretation of the late endosome/lysosome-independent localization of MPR300 to the TGN is that MPR300 does not pass through cholesterol-laden late endosomes during endosome-to-TGN transport. Immunofluorescence data revealed that MPR300 exclusively colocalizes with two TGN markers, AP-1 and syntaxin 6. That both AP-1 (47, 48) and syntaxin 6 (49, 50) localize not only in the TGN but also in early endosomes may account for the transit of MPR300 between these compartments. Indeed, significant redistribution of MPR300 to EEA1-positive early endosomes was observed when cells were treated with chloroquine, which is known to cause the accumulation of TGN38 in early endosomes due to impairment of the retrieval pathway to the TGN (37, 38). In this context, recycling endosomes may also be contained in this pathway, because colocalization between MPR300 and internalized Tfn was seen in cells treated with chloroquine. The same results were also obtained with other cell lines (data not shown). Thus, MPR300 may travel the same route as TGN38 (51) and Shiga toxin B (STxB) (52), both of which have been known to be transported from early/recycling endosomes to the TGN. It has been demonstrated that transport of MPR300 from early endosomes to the TGN is dependent on AP-1 (11). In this regard, it is noteworthy that STxB colocalizes with the γ subunit of AP-1 on early/recycling endosomes (53). On the basis of this evidence and the results presented in this study, we propose that in normal and NPC fibroblasts, MPR300 is exclusively targeted from the TGN to early endosomes, from where it rapidly recycles back to the TGN without being delivered to late endosomes.

Our results are consistent with a previous report that at steady state, most MPR300 was distributed within the TGN
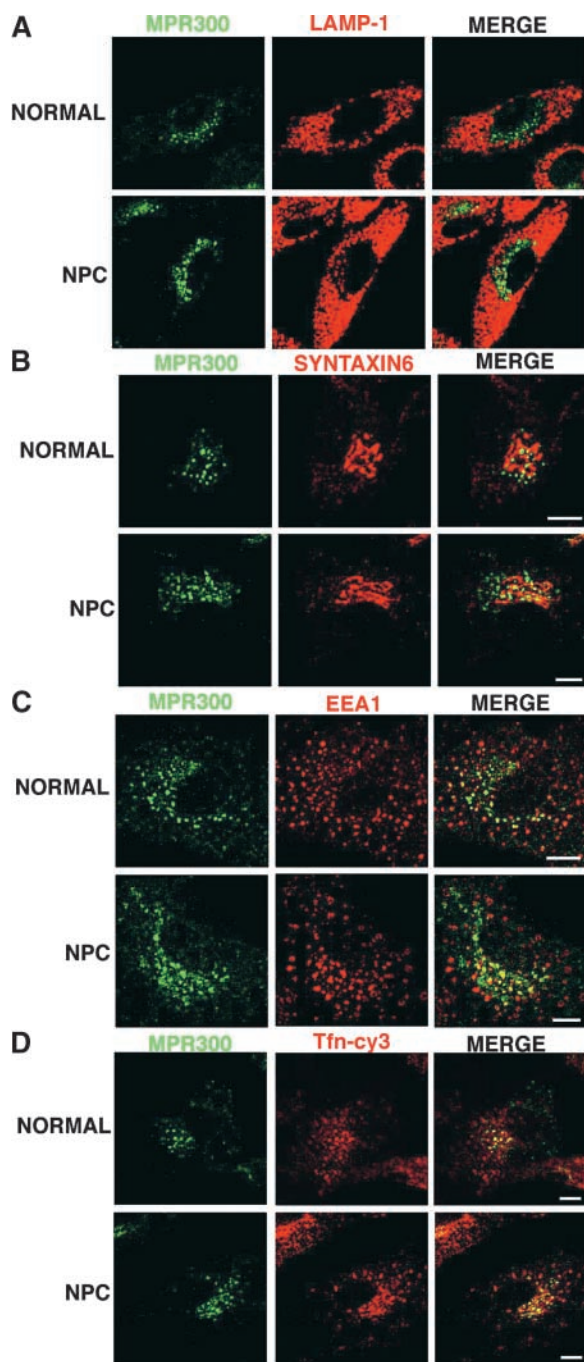
Fig. 10. Effect of chloroquine on the distribution of MPR300 in normal and NPC fibroblasts. Normal and NPC fibroblasts were incubated with 200 μM chloroquine for 3 h, and then cells were fixed, permeabilized, and incubated with anti-MPR300 (A–D, green) and anti-LAMP-1 (A, red), anti-syntaxin 6 (B, red), or anti-EEA1 (C, red). In D, cells were incubated with 200 μM chloroquine for 3 h and internalized Cy3-transferrin for 1 h in the presence of chloroquine. Cells were visualized by confocal microscopy. The right columns show the merged images for triple staining of MPR300 and each organelle marker. Bars = 10 μm.

and in vacuoles in the peripheral cytoplasm, but not in any endosomal compartments lying on the endosome-lysosome pathway (54). In this case, the newly synthesized MPR300 and cathepsin D are delivered to the immature

MVBs, after which the receptor dissociates from the lysosomal enzyme cathepsin D and rapidly leaves. Thus, it is suggested that MPR300-rich vacuoles in the peripheral cytoplasm are on the return route from the Tfn receptor-containing immature MVBs to the TGN. Similarly, a recent study revealed that in the steady state, the bulk of green fluorescence protein (GFP)-tagged MPR300 expressed in HeLa cells localizes to the TGN, peripheral tubulo-vesicular structures, and early endosomes containing internalized Tfn, but is not detected over late endocytic compartments (55). The time-lapse videomicroscopy further showed that GFP-MPR300 exits from the TGN via tubular elements, a process which requires the presence of microtubule and actin networks and is controlled by ARF-1 GTPase, and that GFP-MPR300 containing small tubular elements detached from the TGN can fuse with peripheral tubulo-vesiclular structures as well as early endosomes. However, whether GFP-MPR300 delivered to early endosomes is recycled back to the TGN without passing through late endosomes, as well as the possibility of direct fusion between the TGN-derived tubular elements containing GFP-MPR300 and late endosomes, remains to be determined.

We of course cannot eliminate the possibility that MPR300 rapidly passes through late endosomes during its transport from early endosomes to the TGN. If this is the case, it would lead to an inability to detect MPR300 in late endosomes, because the detection of molecules in compartments in which they localize or transit depends on their resident and passage times. Although there is the notion that MPR300 recycles back to the TGN from late endosomes in a manner dependent on Rab9 and TIP47 (13), this is based on previous results that at steady state, MPR300 predominantly localizes in late endosomes rather than in the TGN (56). In contrast to the phenotypes observed in cells depleted of PACS-1 or AP-1, which revealed the redistribution of MPR300 to early endosomes (10, 11), the antisense depletion of TIP47 has been shown to cause the increased degradation of MPR300 (12). Thus, disruption of MPR300 tail-interacting protein function leads to either retention in early endosomes or degradation of the receptor without an accumulation in late endosomes/lysosomes. These results may also suggest the failure to detect MPR300 in these degradative compartments.

Our findings that at steady state MPR300 is mainly localized to the TGN and is recycled between the TGN and early endosomes, therefore, provide important insights into the definition of late endosomes and therefore the biogenesis of lysosomes, because late endosomes are distinguished from lysosomes by the presence of MPR300. The results from this report, combined with those from other studies, strongly emphasize that MPR300 is not a universal marker for late endosomes. Besides, given that MPR300 is retrieved from early endosomes, how are lysosomal enzymes delivered to lysosomes after being dissociated from MPR300 in early endosomes? This is also important in regard to whether transport between early endosomes and late endosomes is due to a vesicle transport or to maturation of early endosomes. A more careful examination of endosome-to-TGN transport

of MPR300 will be necessary to understand fully this central dogma in lysosome biogenesis.

REFERENCES

1. Ludwig, T., H. Munier-Lehmann, U. Bauer, M. Hollinshead, C. Ovitt, P. Lobel, and B. Hoflack. 1994. Differential sorting of lysosomal enzymes in mannose 6-phosphate receptor-deficient fibroblasts. *EMBO J.* **13:** 3430–3437.

2. Pohlmann, R., M. Wendland, C. Boeker, and K. von Figura. 1995. The two mannose 6-phosphate receptors transport distinct complements of lysosomal enzymes. *J. Biol. Chem.* **270:** 27311–27318.

3. Kornfeld, S. 1992. Structure and function of the mannose 6-phosphate/insulinlike growth factor II receptors. *Annu. Rev. Biochem.* **61:** 307–330.

4. Hille-Rehfeld, A. 1995. Mannose 6-phosphate receptors in sorting and transport of lysosomal enzymes. *Biochim. Biophys. Acta.* **1241:** 177–194.

5. Dell'Angelica, E. C., and G. S. Payne. 2001. Intracellular cycling of lysosomal enzyme receptors: cytoplasmic tails' tales. *Cell.* **106:** 395–398.

6. Boehm, M., and J. S. Bonifacino. 2001. Adaptins: the final recount. *Mol. Biol. Cell.* **12:** 2907–2920.

7. Puertollano, R., R. C. Aguilar, I. Gorshkova, R. J. Crouch, and J. S. Bonifacino. 2001. Sorting of mannose 6-phosphate receptors mediated by the GGAs. *Science.* **292:** 1712–1716.

8. Zhu, Y., B. Doray, A. Poussu, V-P. Lehto, and S. Kornfeld. 2001. Binding of GGA2 to the lysosomal enzyme sorting motif of the mannose 6-phosphate receptor. *Science.* **292:** 1716–1718.

9. Crump, C. M., Y. Xiang, L. Thomas, F. Gu, C. Austin, S. A. Tooze, and G. Thomas. 2001. PACS-1 binding to adaptors is required for acidic cluster motif-mediated protein traffic. *EMBO J.* **20:** 2191–2201.

10. Wan, L., S. S. Molloy, L. Thomas, G. Liu, Y. Xiang, S. L. Rybak, and G. Thomas. 1998. PACS-1 defines a novel gene family of cytosolic sorting proteins required for *trans*-Golgi network localization. *Cell.* **94:** 205–216.

11. Meyer, C., D. Zizioli, S. Lausmann, E-L. Eskelinen, J. Hamann, P. Saftig, K. von Figura, and P. Schu. 2000. μ1A-adaptin-deficient mice: lethality, loss of AP-1 binding and rerouting of mannose 6-phosphate receptors. *EMBO J.* **19:** 2193–2203.

12. Diaz, E., and S. R. Pfeffer. 1998. TIP47: a cargo selection device for mannose 6-phosphate receptor trafficking. *Cell.* **93:** 433–443.

13. Carroll, K. S., J. Hanna, I. Simon, J. Krise, P. Barbero, and S. R. Pfeffer. 2001. Role of rab9 GTPase in facilitating receptor recruitment by TIP47. *Science.* **292:** 1373–1376.

14. Kobayashi, T., M-H. Beuchat, M. Lindsay, S. Frias, R. D. Palmiter, H. Sakuraba, R. G. Parton, and J. Gruenberg. 1999. Late endosomal membranes rich in lysobisphosphatidic acid regulate cholesterol transport. *Nat. Cell Biol.* **1:** 113–118.

15. Ohashi, M., I. Miwako, A. Yamamoto, and K. Nagayama. 2000. Arrested late endosome-lysosome intermediate aggregate observed in a Chinese hamster ovary cell mutant, LEX2, isolated by repeated flow-cytometric cell sorting. *J. Cell Sci.* **113:** 2187–2205.

16. Miwako, I., A. Yamamoto, T. Kitamura, K. Nagayama, and M. Ohashi. 2001. Cholesterol requirement for cation-independent mannose 6-phosphate receptor exit from multivesicular late endosomes to the Golgi. *J. Cell Sci.* **114:** 1765–1776.

17. Ory, D. S. 2000. Niemann-Pick type C: a disorder of cellular cholesterol trafficking. *Biochim. Biophys. Acta.* **1529:** 331–339.

18. Liscum, L. 2000. Niemann-Pick type C mutations cause lipid traffic jam. *Traffic.* **1:** 218–225.

19. Brown, W. J., D. B. DeWald, S. D. Emr, H. Plutner, and W. E. Balch. 1995. Role for phosphatidylinositol 3-kinase in the sorting and transport of newly synthesized lysosomal enzymes in mammalian cells. *J. Cell Biol.* **130:** 781–796.

20. Davidson, H. W. 1995. Wortmannin causes mistargeting of procathepsin D. Evidence for the involvement of a phosphatidylinositol 3-kinase in vesicle transport to lysosomes. *J. Cell Biol.* **130:** 797–805.

21. Row, P. E., B. J. Reaves, J. Domin, J. P. Luzio, and H. W. Davidson. 2001. Overexpression of a rat kinase-deficient phosphatidylinositide 3-kinase, Vps34p, inhibits cathepsin D maturation. *Biochem. J.* **353:** 655–661.

22. Kuronita, T., E-L. Eskelinen, H. Fujita, P. Saftig, M. Himeno, and Y. Tanaka. 2002. A role for the lysosomal membrane protein LGP85 in the biogenesis and maintenance of endosomal and lysosomal morphology. *J. Cell Sci.* **115:** 4117–4131.

23. Sahagian, G. G., J. Distler, and G. W. Jourdian. 1982. Membrane receptor for phosphomannosyl residues. *Methods Enzymol.* **83:** 392–396.

24. Köster, A., K. von Figura, and R. Pohlmann. 1994. Mistargeting of lysosomal enzymes in Mr 46000 mannose 6-phosphate receptor-deficient mice is compensated by carbohydrate-specific endocytotic receptors. *Eur. J. Biochem.* **224:** 685–689.

25. Porter, M. T., A. L. Fluharty, and H. Kihara. 1969. Metachromatic leukodystrophy: arylsulfatase-A deficiency in skin fibroblast cultures. *Proc. Natl. Acad. Sci. USA.* **62:** 887–891.

26. Barrett, A. J., and H. Kirschke. 1981. Cathepsin B, cathepsin H, and cathepsin L. *Methods Enzymol.* **80:** 535–561.

27. Tanaka, Y., R. Tanaka, T. Kawabata, Y. Noguchi, and M. Himeno. 2000. Lysosomal cysteine protease, cathepsin B, is targeted to lysosomes by the mannose 6-phosphate-independent pathway in rat hepatocytes: site-specific phosphorylation in oligosaccharides of the proregion. *J. Biochem.* **128:** 39–48.

28. Tanaka, Y., R. Tanaka, and M. Himeno. 2000. Lysosomal cysteine protease, cathepsin H, is targeted to lysosomes by the mannose 6-phosphate-independent system in rat hepatocytes. *Biol. Pharm. Bull.* **23:** 805–809.

29. Laemmli, U. K. 1970. Cleavage of structural protein during the assembly of the head of bacteriophage T4. *Nature.* **227:** 680–685.

30. Besley, G. T. N., and S. E. Moss. 1983. Studies of sphingomyelinase and β-glucosidase activities in Niemann-Pick disease variants: phosphodiesterase activities measured with natural and artificial substrates. *Biochim. Biophys. Acta.* **752:** 54–64.

31. Thomas, G. H., C. M. Tuck-Muller, C. S. Miller, and L. W. Reynolds. 1989. Correction of sphingomyelinase deficiency in Niemann-Pick type C fibroblasts by removal of lipoprotein fraction from culture media. *J. Inherit. Metab. Dis.* **12:** 139–151.

32. Rohrer, J., A. Schweizer, K. F. Johnson, and S. Kornfeld. 1995. A determinant in the cytoplasmic tail of the cation-dependent mannose 6-phosphate receptor prevents trafficking to lysosomes. *J. Cell Biol.* **130:** 1297–1306.

33. Liscum, L., and J. R. Faust. 1989. The intracellular transport of low density lipoprotein-derived cholesterol is inhibited in Chinese hamster ovary cells cultured with 3-beta-[2-(diethylamino)ethoxy]androst-5-en-17-one. *J. Biol. Chem.* **264:** 11796–11806.

34. Neufeld, E. B., M. Wastney, S. Patel, S. Suresh, A. M. Cooney, N.K. Dwyer, C. F. Roff, K. Ohno, J. A. Morris, E. D. Carstea, J. P. Incardona, J. F. Strauss III, M. T. Vanier, M. C. Patterson, R. O. Brady, P. G. Pentchev, and E. J. Blanchette-Mackie. 1999. The Niemann-Pick C1 protein resides in a vesicular compartment linked to retrograde transport of multiple lysosomal cargo. *J. Biol. Chem.* **274:** 9627–9635.

35. Cruz, J. C., S. Sugii, C. Yu, and T. Y. Chang. 2000. Role of Niemann-Pick type C1 protein in intracellular trafficking of low density lipoprotein-derived cholesterol. *J. Biol. Chem.* **275:** 4013–4021.

36. Lange, Y., J. Ye, M. Rigney, and T. Steck. 2000. Cholesterol movement in Niemann-Pick type C cells and in cells treated with amphiphiles. *J. Biol. Chem.* **275:** 17468–17475.

37. Reaves, B. J., G. Banting, and J. P. Luzio. 1998. Lumenal and transmembrane domains play a role in sorting type I membrane proteins on endocytic pathways. *Mol. Biol. Cell.* **9:** 1107–1122.

38. Rous, B. A., B. J. Reaves, G. Ihrke, J. A. G. Briggs, S. R. Gray, D. J. Stephens, G. Banting, and J. P. Luzio. 2002. Role of adaptor complex AP-3 in targeting wild-type and mutated CD63 to lysosomes. *Mol. Biol. Cell.* **13:** 1071–1082.

39. Frolov, A., K. Srivastava, D. Daphna-Iken, L. M. Traub, J. E. Schaffer, and D. S. Ory. 2001. Cholesterol overload promotes morphogenesis of a Niemann-Pick C (NPC)-like compartment independent of

inhibition of NPC1 or HE1/NPC2 function. *J. Biol. Chem.* **276:** 46414–46426.

40. Kobayashi, T., E. Stang, K. S. Fang, P. de Moerloose, R. G. Parton, and J. Gruenberg. 1998. A lipid associated with the antiphospholipid syndrome regulates endosome structure and function. *Nature.* **392:** 193–197.

41. Ko, D. C., M. D. Gordon, G. J. Jin, and M. P. Scott. 2001. Dynamic movements of organelles containing Niemann-Pick C1 protein: NPC1 involvement in late endocytic events. *Mol. Biol. Cell.* **12:** 601–614.

42. Higgins, M. E., J. P. Davies, F. W. Chen, and Y. A. Ioannou. 1999. Niemann-Pick C1 is a late endosome-resident protein that transiently associates with lysosomes and the trans-Golgi network. *Mol. Genet. Metab.* **68:** 1–13.

43. Zhang, M., N. K. Dwyer, D. C. Love, A. Cooney, M. Comly, E. B. Neufeld, P. G. Pentchev, E. J. Blanchette-Mackie, and J. A. Hanover. 2001. Cessation of rapid late endosomal tubulovesicular trafficking in Niemann-Pick type C1 disease. *Proc. Natl. Acad. Sci. USA.* **98:** 4466–4471.

44. Zhang, M., N. K. Dwyer, E. B. Neufeld, D. C. Love, A. Cooney, M. Comly, S. Patel, H. Watari, J. F. Strauss III, P. G. Pentchev, J. A. Hanover, and E. J. Blanchette-Mackie. 2001. Sterol-modulated glycolipid sorting occurs in Niemann-Pick C1 late endosomes. *J. Biol. Chem.* **276:** 3417–3425.

45. Choudhury, A., M. Dominguez, V. Puri, D. K. Sharma, K. Narita, C. L. Wheatley, D. L. Marks, and R. E. Pagano. 2002. Rab proteins mediate Golgi transport of caveola-internalized glycosphingolipids and correct lipid trafficking in Niemann-Pick C cells. *J. Clin. Invest.* **109:** 1541–1550.

46. Walter, M., J. P. Davies, and Y. A. Ioannou. 2003. Telomerase immortalization upregulates Rab9 expression and restores LDL cholesterol egress from Niemann-Pick C1 late endosomes. *J. Lipid Res.* **44:** 243–253.

47. Hirst, J., and M. S. Robinson. 1998. Clathrin and adaptors. *Biochim. Biophys. Acta.* **1404:** 173–193.

48. Futter, C. E., A. Gibson, E. H. Allchin, S. Maxwell, L. J. Ruddock, G. Odorizzi, D. Domingo, I. S. Trowbridge, and C. R. Hopkins. 1998. In polarized MDCK cells basolateral vesicles arise from clathrin-γ-adaptin-coated domains on endosomal tubules. *J. Cell Biol.* **141:** 611–623.

49. Bock, J. B., R. C. Lin, and R. H. Scheller. 1996. A new syntaxin family member implicated in targeting of intracellular transport vesicles. *J. Biol. Chem.* **271:** 17961–17965.

50. Bock, J. B., J. Klumperman, S. Davanger, and R. H. Scheller. 1997. Syntaxin 6 functions in trans-Golgi network vesicle trafficking. *Mol. Biol. Cell.* **8:** 1261–1271.

51. Ghosh, R. N., W. G. Mallet, T. T. Soe, T. E. McGraw, and F. R. Maxfield. 1998. An endocytosed TGN38 chimeric protein is delivered to the TGN after trafficking through the endocytic recycling compartment in CHO cells. *J. Cell Biol.* **142:** 923–936.

52. Mallard, F., D. Tenza, C. Antony, J. Salamero, B. Goud, and L. Johannes. 1998. Direct pathway from early/recycling endosomes to the Golgi apparatus revealed through the study of Shiga toxin B-fragment transport. *J. Cell Biol.* **143:** 973–990.

53. Mallard, F., B. L. Tang, T. Galli, D. Tenza, A. Saint-Pol, X. Yue, C. Antony, W. Hong, B. Goud, and L. Johannes. 2002. Early/recycling endosomes-to-TGN transport involves two SNARE complexes and a Rab6 isoform. *J. Cell Biol.* **156:** 653–664.

54. Hirst, J., C. E. Futter, and C. R. Hopkins. 1998. The kinetics of mannose 6-phosphate receptor trafficking in the endocytic pathway in Hep-2 cells: the receptor enters and rapidly leaves multivesicular endosomes without accumulating in a prelysosomal compartment. *Mol. Biol. Cell.* **9:** 809–816.

55. Waguri, S., F. Dewitte, R. Le Borgne, Y. Rouillé, Y. Uchiyama, J-F. Dubremetz, and B. Hoflack. 2003. Visualization of TGN to endosome trafficking through fluorescently labeled MPR and AP-1 in living cells. *Mol. Biol. Cell.* **14:** 142–155.

56. Griffiths, G., B. Hoflack, K. Simons, I. Mellman, and S. Kornfeld. 1988. The mannose 6-phosphate receptor and the biogenesis of lysosomes. *Cell.* **52:** 329–341.